

Efficiency of the Satellite Retrieval of Mean Virtual Temperatures as a Function of Layer Thickness

HENRY E. FLEMING AND DAVID S. CROSBY*

Satellite Research Laboratory, NOAA/NESDIS, Washington, DC

MITCHELL D. GOLDBERG**

ST Systems Corporation (STX), Lanham, Maryland

28 August 1989 and 27 January 1991

ABSTRACT

Layer-mean virtual temperatures retrieved from satellite measurements are more accurate than retrievals at specific pressures, not only because an averaging process is involved, but also because of advantages in the retrieval process. In this note, a "retrieval efficiency" is derived to express this advantage over simple averaging as a function of layer thickness. The efficiency is examined for two common cases of retrieval initial guess: a statistical sample mean and a forecast profile obtained from a numerical prediction model. The advantage of the layer-mean retrieval clearly is demonstrated in both cases.

1. Introduction

It is the purpose of this note to illustrate how the accuracy of the satellite-retrieved mean virtual temperature improves with layer thickness above and beyond improvement due to the vertical averaging. To separate the improvement in accuracy due to the averaging process from that due to the retrieval process itself, we normalize the problem by dividing out the contribution due to averaging. This yields a measure of retrieval efficiency that is discussed in detail in the following.

We begin by providing an appropriate mathematical formalism for quantifying retrieval efficiency based on the so-called "minimum variance simultaneous" method of solution of the retrieval problem. It is shown that this method of solution lends itself in a natural way to calculating the mean virtual temperature by means of an averaging vector. (However, the approach is sufficiently general that it applies to other linear methods of solution as well.) Then the formula for calculating the retrieval efficiency is developed and curves showing the results are presented. An interpretation and discussion of these curves is given.

* Permanent affiliation is with the American University, Washington, DC.

** Now affiliated with the Satellite Research Laboratory, NOAA/NESDIS.

Corresponding author address: Henry E. Fleming, NOAA/NESDIS, 5200 Auth Road, Washington, DC 20233.

Finally, there is a great deal of interest, activity, and even controversy in using forecast temperatures from an NWP model as the initial guess in the retrieval process and applying the retrieved temperature profiles to a retrieval/analysis/forecast interactive system. We infer from our results on retrieval efficiency that the interactive retrieval approach is useful.

For a related paper that analyzes retrieval error components, one should see Rodgers (1990).

2. Methodology

To develop the required mathematical formalism, we briefly review the minimum variance simultaneous (MVS) temperature/moisture retrieval scheme used operationally by the NESDIS (see Fleming et al. 1986). We begin with the linearized, discrete form of the radiative transfer equation

$$\mathbf{r} = \mathbf{A}\mathbf{v} + \boldsymbol{\epsilon} \quad (1)$$

where \mathbf{r} is the m -dimensional vector of measured radiances, \mathbf{A} is the matrix of weighting (or kernel) functions, \mathbf{v} is the solution vector, and $\boldsymbol{\epsilon}$ is the vector of measurement errors that are assumed to be independent of \mathbf{v} . The vector \mathbf{v} is a 132-element temperature-moisture vector of the form

$$\mathbf{v} = (t_1, \dots, t_{100}, t_s, q_1, \dots, q_{31})^T \quad (2)$$

where t_i is the atmospheric temperature at pressure level p_i (with $p_1 = 0.01$ mb and $p_{100} = 1000$ mb), t_s is the surface skin temperature, q_j is the water-vapor mixing ratio at pressure level p_j (with $p_1 = 300$ mb and p_{31}

= 1000 mb), and the superscript T denotes the transpose.

Let v_0 be the initial approximation (i.e., the initial guess) to v , let $r_0 = Av_0$ be the initial guess for r , and let C be the $132 \times m$ retrieval coefficient matrix. Then the MVS solution is given by

$$v^{\wedge} = v_0 + C(r - r_0) \tag{3}$$

where

$$C = S_v A^T (AS_v A^T + S_e)^{-1} \tag{4}$$

and where S_v is the covariance matrix of the solution vector, S_e is the covariance matrix of the error vector, and the superscript -1 denotes the matrix inverse. Admittedly, the matrix A in (1) is nonlinear in that it is evaluated for the initial vector v_0 . However, for the purposes of this note, v_0 is a sufficiently good approximation to v that the operator C can be treated as being linear in (3) and (4).

A simple method for deriving mean virtual temperatures from the vector v of (2) now is developed as follows. Recall that the virtual temperature t^* at any level in the atmosphere can be approximated from the temperature t and water-vapor mixing ratio q by the formula

$$t^* = t + q/6. \tag{5}$$

To determine the mean virtual temperature \bar{t}^* over a layer bounded by pressures p_i at the top and p_{i+k} at the bottom, define a boxcar function in vector form as follows:

$$b = [0, \dots, 0, \underbrace{1, \dots, 1}_{k \text{ times}}, 0, \dots, 0, \underbrace{1/6, \dots, 1/6, 0, \dots, 0}_{k \text{ times}}]^T/k \tag{6}$$

where a member of the set of k vector elements $1/6$ will not appear if its corresponding pressure is less than 300 mb, since these elements correspond to the water-vapor mixing ratios in (2). Then one obtains a simple and direct formula for \bar{t}^* from (5) by taking the dot product of vectors b of (6) and v of (2), i.e.,

$$\bar{t}^* = b^T v. \tag{7}$$

Note that if either of the pressure boundaries for \bar{t}^* do not coincide with the indexed pressure levels dictated by the vector (2), the approach is still valid. All that needs to be done is to determine the fractional interpolation weight values for the pressures and then insert these values in the appropriate positions of the boxcar vector (6) and also add them to k in the denominator of (6).

To arrive at an expression of retrieval efficiency as a function of layer thickness, one more set of intermediate formulas is needed. Recall that if random vectors x and y have the linear relationship $y = Bx$, then

the associated covariance matrices S_y and S_x have the relationship $S_y = BS_x B^T$. It follows that the covariance matrices S_r and $S_{v^{\wedge}}$ of the vectors r and v^{\wedge} of (1) and (3), respectively, are given by

$$S_r = AS_v A^T + S_e \tag{8}$$

and

$$S_{v^{\wedge}} = CS_e C^T, \tag{9}$$

which by (4) and (8) become

$$S_{v^{\wedge}} = S_v A^T (AS_v A^T + S_e)^{-1} AS_v. \tag{10}$$

By the same argument, the variance of the scalar \bar{t}^* of (7) is

$$\sigma^2 = b^T S_{v^{\wedge}} b, \tag{11}$$

while the approximation \bar{t}^{\wedge} of \bar{t}^* , which is

$$\bar{t}^{\wedge} = b^T v^{\wedge}, \tag{12}$$

has the scalar variance

$$(\sigma^*)^2 = b^T S_{v^{\wedge}} b \tag{13}$$

where $S_{v^{\wedge}}$ is given explicitly by (10). By using various combinations of unit elements, and associated elements $1/6$, in the boxcar vector b of (6), one can study how the σ 's in (11) and (13) change with the pressure boundaries of the various layers formed by b .

The particular significance of the scalar (11) is that it represents the variance of the original (initial) mean virtual temperature data, i.e., before any satellite radiance measurements are involved. On the other hand, the scalar (13) represents the variance of the mean virtual temperature that is retrieved by the minimum variance simultaneous estimator. Of course, the σ 's of (11) and (13) are a function of the layer dictated by the boxcar vector b .

It follows from the discussion of the previous paragraph that the retrieval efficiency, denoted by the scalar e , can be defined as the ratio of the variances of the two mean virtual temperatures, i.e.,

$$e = (\sigma^*/\sigma)^2 = (b^T S_{v^{\wedge}} b)(b^T S_v b)^{-1}. \tag{14}$$

The index e is very similar in meaning to the fractional reduction in variance and to the coefficient of multiple determination in regression analysis.

As indicated in section 1, much of the change in σ^* and σ with increasing layer thickness is due to the implicit averaging process. However, by using quadratic forms involving the boxcar vector b in both the numerator and denominator of (14), the averaging process is effectively eliminated. Thus, the retrieval efficiency index is a measure of the improvement in mean virtual temperature accuracy due exclusively to the retrieval process, since it compares the mean virtual temperature information added by the satellite radiance observations to the total information to be retrieved initially for the layer in question.

3. Results

Using Eq. (14), we can determine the virtual temperature retrieval efficiency for various layer configurations and meteorological conditions. The meteorological conditions are varied in (14) by changing the covariance matrix \mathbf{S}_p in (10) and (14). In order to linearize (10), we based the weighting function matrix \mathbf{A} on the mean temperature–moisture profile associated with \mathbf{S}_p .

The transmittance data used to generate the matrix \mathbf{A} in (10) are for 16 channels of the TIROS Operational Vertical Sounder (TOVS). In particular, we used channels 2, 3, 4, 5, 6, 7, 13, 14, 15, and 16 of the High-Resolution Infrared Radiation Sounder, version 2 (HIRS/2); the three Stratospheric Sounder Unit (SSU) channels; and channels 2, 3, and 4 of the Microwave Sounder Unit (MSU). Consequently, the matrix \mathbf{A} has dimensions 16×132 . Tables giving the characteristics of the TOVS channels and descriptions of the TOVS instruments can be found in Schwalb (1978) and Smith et al. (1979). The transmittance functions were generated using the models described in Weinreb et al. (1981).

The error covariance matrix \mathbf{S}_e in (10) is based on the overall system error, not just on the instrumental noise values. It has been found empirically (Fleming et al. 1985) that error correlations exist among channels, and that an appropriate way to represent these correlations is to use a (partially) tridiagonal matrix for \mathbf{S}_e . The nonzero entries of \mathbf{S}_e represent typical system error values.

The data used to generate covariance matrices \mathbf{S}_p are a global compilation of radiosonde temperature/moisture profiles for the year 1983. The 1-yr dataset was divided into 12 subsets covering the 4 seasons and the following 3 latitudinal belts: a tropical belt from 30°S to 30°N , a midlatitudinal belt from 30° to 60°N , and a polar belt from 60° to 90°N . Because of its sparseness, data in the Southern Hemisphere were not used. A temperature–moisture covariance matrix \mathbf{S}_p and its associated mean temperature–moisture profile \mathbf{v}_0 was calculated for each of these 12 subsets.

Since the objective of this note is to draw inferences about the efficiency of the MVS retrieval of mean virtual temperatures as a function of layer thickness, we find it sufficient to discuss only 1 of the 12 cases. The fall midlatitudinal case (sample size 221) was chosen because it has the largest initial temperature variance. While the other cases produce different results, the gross features are sufficiently similar so that nothing is gained by including them in the discussion.

A second and very different case also is included in this study. It was mentioned at the end of section 1 that there currently is much activity in developing retrieval/analysis/forecast interactive systems. To determine the retrieval efficiency of this kind of system, we generated a covariance matrix of the “forecast error” by compiling vertical temperature–moisture profile dif-

ferences between the National Meteorological Center 6-h forecast from the medium-range forecast model and radiosonde temperature–moisture profiles whenever the two kinds of profiles coincided in time and place.

This was done globally for several days during the month of August 1990, which produced a sample size in excess of 2000. A single global covariance matrix was computed from these data, which is referred to as the “global forecast case.” When computing the various quantities needed for this case, the instrumental and noise characteristics, along with the transmittance data, were the same as those described previously. An average radiosonde profile computed from the set was used to evaluate the weighting function matrix \mathbf{A} used in (4), (8), and (10).

Results from applying the fall midlatitudinal and global forecast covariance matrices to (10) and (14) are shown in Figs. 1 and 2, respectively. Linear increments of the ordinate, in both of the figures, are in units of pressure to the two-sevenths power. The families of curves in Figs. 1 and 2 represent the retrieval efficiency e as a percent. The curves can be interpreted as being that fraction of the initial mean virtual temperature variance that actually was retrieved for the layer thickness indicated. In both figures, the results are shown as a function of the following thicknesses: the solid curve is for zero thickness (i.e., for point values) and the four curves with symbols are for constant thicknesses of 1, 3, 5, and 9 km, as indicated. The thicknesses were computed by applying (7) to \mathbf{v}_0 and multiplying each result by 29.28 m K^{-1} times the logarithm of the ratio of the bottom boundary pressure to the top one.

The solid point-value curves in Figs. 1 and 2 are self-explanatory, but the remaining four curves require clarification. Each symbol on these curves represents the pressure location of the middle of the layer having the thickness indicated. It is clear from the spacing of the symbols that the layers are not stacked one on top of the other, but overlap. This allows one to determine the retrieval efficiency continuously for all pressures between 50 and 1000 mb without regard to the thickness of the layer. Furthermore, the bottommost symbol of each curve moves upward as the layers get thicker, because all thickness calculations start at 1000 mb. Thus, for example, in Fig. 1 the bottommost 1-km layer is centered at 941 mb, while the bottommost 9-km layer is centered at 551 mb.

4. Discussion

It is immediately apparent from Fig. 1 that the tropopause region is the most difficult part of the vertical temperature profile to retrieve for all layer thicknesses. This result is just what one would expect from prior experience. However, a result that is perhaps unex-

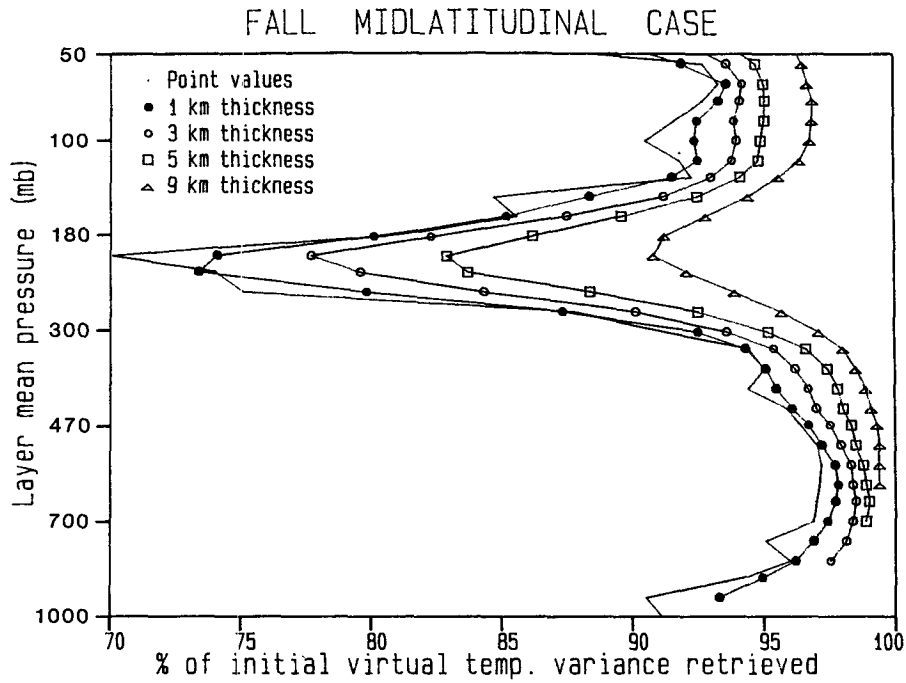


FIG. 1. The retrieval efficiency of the mean virtual temperature as a function of pressure for the layer thickness indicated for the fall midlatitudinal data subset.

pected is the large, progressive improvement in efficiency with increasing layer thicknesses. We know that both the retrieved and initial variances decrease with

increasing layer thickness, because of increased averaging. One might expect both of these variances to decrease at about the same rate and, hence, their ratio

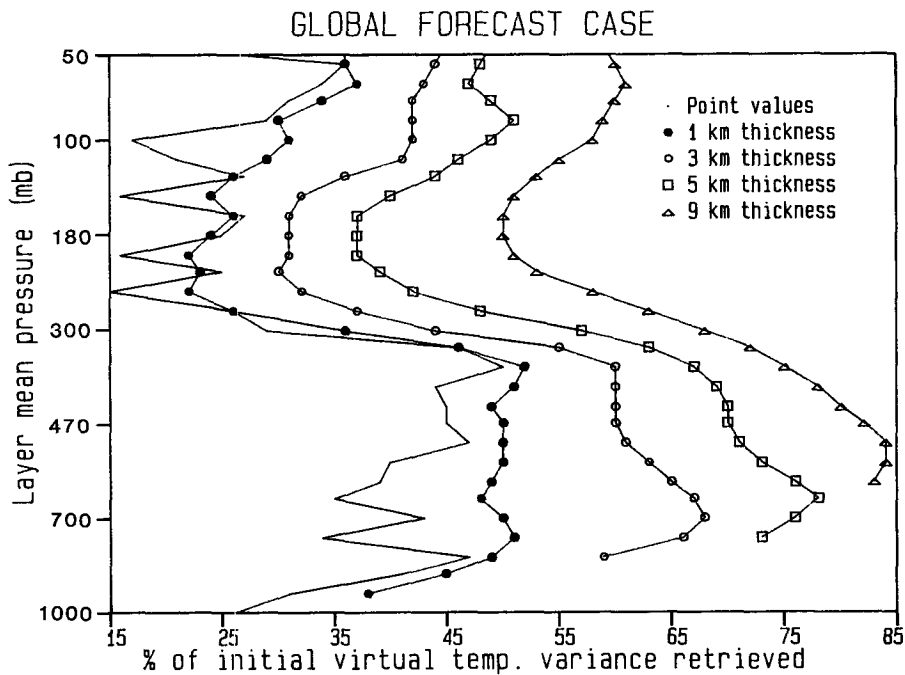


FIG. 2. The retrieval efficiency of the mean virtual temperature as a function of pressure for the layer thickness indicated for the global radiosonde-forecast dataset.

(the retrieval efficiency) to remain nearly constant. But clearly, the retrieved variance is decreasing more slowly than the initial variance.

We assume that this phenomenon is related to the structure of the retrieved profiles. We know that as the layer thicknesses increase, the profiles of temperature averages become smoother. Apparently, as the profiles become smoother, they become increasingly easy to retrieve and, hence, the retrieved variance tends to increase. On the other hand, the denominator is affected only by the boxcar vectors and not by the retrieval process. Hence, the variance of the numerator decreases more slowly than that of the denominator.

Another phenomenon worth noting in Fig. 1 is the varying rates at which the retrieval efficiency improves with increasing layer thickness. For example, the point retrieval at its most inefficient point value (i.e., 0-km thickness) is only 70% efficient, while the 9-km thickness retrieval centered at this same point is 91% efficient. At the other extreme, the point retrieval at its most efficient point value is 92% efficient, while at the 9-km thickness it is 99% efficient. Thus, the improvement in efficiency with increasing thickness is a function of the initial efficiency.

The percentages just cited can be interpreted another way. From (14) it is clear that the quantity $(1 - e)$ is a measure of the fractional variance error of the mean virtual temperature due to the retrieval process, since the numerator is the difference between the total variance to be retrieved and the variance that was retrieved. Thus, returning to our previous examples, we see that the most inefficiently retrieved point value has an error of 30%, while the 9-km retrieval centered at this point has an error of only 9%. At the other extreme, the retrieval at its most efficient point value has an error of 8%, while at the 9-km thickness the error is 1%. In short, this means that as the layers get thicker, it is easier to improve a poor retrieval than it is to improve a good retrieval.

This last conclusion is strongly reinforced by Fig. 2, particularly when one notes the very different scale of the abscissa in Fig. 2 as compared to Fig. 1. All of the other discussion about Fig. 1 holds as well for Fig. 2. In particular, the retrieval efficiency increases with increasing layer thickness as before, and most likely for the reason cited.

We also note in Figs. 1 and 2 that not only is the efficiency increased with increasing thickness, but also the thicker the designated layer is, the smoother the associated efficiency curve is, and the greater the tendency toward the curve becoming a vertical straight line.

The argument has been advanced that since the satellite radiance measurements are, in a sense, mean temperatures over deep layers as represented by the associated weighting functions, there should be optimal thicknesses for which the retrieval errors are minimal. Figures 1 and 2 obviously dispute this hypothesis in

that the efficiency, and, hence, the retrieval accuracy, increase indefinitely with increasing layer thickness. This is due to the overlap (i.e., the interdependence) of the weighting functions.

Finally, we discuss the obvious discrepancy between Figs. 1 and 2; namely, that the general level of retrieval efficiency of the global forecast case is much less than that of the fall midlatitudinal case. The reason is that the covariance matrix used for Fig. 1 is computed from the differences between the individual radiosonde profiles in the ensemble and the single associated ensemble mean profile, whereas the covariance matrix used for Fig. 2 is computed from differences between the individual forecasts and the associated individual radiosonde profiles. This results in the individual initial guesses used to produce Fig. 2, being much more accurate than the single initial guess used to produce Fig. 1. Consequently, the large drop in retrieval efficiency observed when comparing Fig. 1 with Fig. 2 is due to a large increase in accuracy of the initial-guess profiles. Thus, it is clear that retrievals with low initial-guess accuracy are more efficient than those with high initial-guess accuracy.

5. Summary and conclusions

A retrieval efficiency index e has been established in section 2 using the ratio (14) of the retrieved to the initial layer-mean virtual temperature variances. This ratio formula was used to minimize the effects due solely to averaging over a layer. The results are shown in Figs. 1 and 2.

The conclusions drawn from the discussion of section 4 can be briefly summarized as follows:

- (i) The retrieval efficiency increases progressively with increasing layer thickness.
- (ii) The retrieval efficiency increases more rapidly with increasing layer thickness when the initial efficiency is low than when it is high. Stated another way, this means that it is easier to improve a poor retrieval than it is to improve a good retrieval by using thicker layers.
- (iii) The thicker the designated layer is, the smoother the associated efficiency curve is and the greater the tendency toward the curve becoming a vertical straight line.
- (iv) Retrievals for any given, fixed-layer thickness having poor initial guesses are more efficient than those having good initial guesses.

These conclusions can be used to assess the procedure of using forecast temperatures from an NWP model as the initial guess in the retrieval process and applying the retrieved temperature profiles to a retrieval/analysis/forecast interactive system (cf., Daniels et al. 1989). Clearly, deeper layers contribute to increased retrieval efficiency. One should then use the deepest layer consistent with the model. In other words,

retrievals should be made in the model-layer framework for maximum efficiency. Point retrievals, which are currently used, are the worst things that one can use in such a system.

Finally, conclusion (iv) suggests that one should realize the greatest improvement in retrieval efficiency (and, hence, in retrieval accuracy) at locations where the forecast is poor and the least improvement in locations where the forecast is good. In other words, the interactive system should perform best where it is needed most and essentially should not alter the forecast where the forecast is good. This is precisely the strategy needed for an effective data assimilation system.

Acknowledgments. The authors are grateful for the useful comments and suggestions by Dr. Eugenia Kalnay and Dr. Lev Gandin of the National Meteorological Center, National Weather Service.

REFERENCES

- Daniels, J. M., M. D. Goldberg, H. E. Fleming, B. Katz, W. E. Baker and D. G. Deaven, 1989: A satellite retrieval-forecast model interactive assimilation system. *Proc. 12th Conf. on Weather Analysis and Forecasting*, Monterey, Amer. Meteor. Soc., 407-411.
- Fleming, H. E., D. S. Crosby and M. D. Goldberg, 1985: Satellite temperature retrievals via the minimum variance solution when the operator is in error. Part 1: Implementation. *Proc. Ninth Conference on Probability and Statistics in Atmospheric Sciences*, Virginia Beach, Amer. Meteor. Soc., 355-357.
- , M. D. Goldberg and D. S. Crosby, 1986: Minimum variance simultaneous retrieval of temperature and water vapor from radiance measurements. *Proc. Second Conference on Satellite Meteorology—Remote Sensing and Applications*, Williamsburg, Amer. Meteor. Soc., 20-23.
- Rodgers, C. D., 1990: Characterization and error analysis of profiles retrieved from remote sounding measurements. *J. Geophys. Res.*, **95**, 5587-5595.
- Schwalb, A., 1978: The TIROS-N/NOAA A-G satellite series. NOAA Tech. Memo. NESS 95, National Oceanic and Atmospheric Administration, Washington, DC, 75 pp.
- Smith, W. L., H. M. Woolf, C. M. Hayden, D. Q. Wark and L. M. McMillin, 1979: The TIROS-N operational vertical sounder. *Bull. Amer. Meteor. Soc.*, **60**, 1177-1187.
- Weinreb, M. P., H. E. Fleming, L. M. McMillin and A. C. Neundorfer, 1981: Transmittances for the TIROS operational vertical sounder. NOAA Tech. Rept. NESS 85, National Oceanic and Atmospheric Administration, Washington, DC, 60 pp.